

Dynamical decoupling induced renormalization of the non-Markovian dynamics

Pochung Chen

Department of Physics, National Tsing-Hua University, Hsinchu 100, Taiwan

(Dated: August 9, 2018)

In this work we develop a numerical framework to investigate the renormalization of the non-Markovian dynamics of an open quantum system to which dynamical decoupling is applied. We utilize a non-Markovian master equation which is derived from the non-Markovian quantum trajectories formalism. It contains incoherent Markovian dynamics and coherent Schrödinger dynamics as its limiting cases and is capable of capture the transition between them. We have performed comprehensive simulations for the cases in which the system is either driven by the Ornstein-Uhlenbeck noise or is described by the spin-boson model. The renormalized dynamics under bang-bang control and continuous dynamical decoupling are simulated. Our results indicate that the renormalization of the non-Markovian dynamics depends crucially on the spectral density of the environment and the envelop of the decoupling pulses. The framework developed in this work hence provides an unified approach to investigate the efficiency of realistic decoupling pulses. This work also opens a way to further optimize the decoupling via pulse shaping.

I. INTRODUCTION

It is known that dynamical decoupling[1, 2, 3, 4] is one of the essential control tools in fighting the decoherence of an open quantum system. In recent years many methods have been developed to design the decoupling pulses. Those methods are based on the group structure or the geometric perspective of the system environment interaction [3, 4, 5, 6, 7, 8]. The effect of a general environment, however, is usually neglected. Dynamical decoupling can be divided into several categories. It can be deterministic and periodic[1, 9], deterministic and concatenated[10], or random[8, 11]. The strength of the pulses can be unbounded, which is usually termed bang-bang decoupling, or bounded [5, 6]. Bounded control uses more realistic control resources and is more tolerant against implementation errors. Both unbounded and bounded control attain the desired decoupling in the ideal limit where the period of a single decoupling cycle approaches zero. In practice, however, the duration of the cycle is finite and there will always be residual decoherence. To the best of our knowledge it is difficult to calculate the exact residual decoherence, especially when the effect of a general environment are taken into account. For a general configuration the amount of residual decoherence might depend on the shape of the decoupling pulses as well as the spectral density of the environment. For example, it has been argued that the bang-bang decoupling might be more efficient when the environment is characterized by the $1/f$ noise in stead of an Ohmic bosonic environment[12, 13]. Recently the effect of a general environment is studied, but only unbounded control are investigated[14]. In other words, a comprehensive study of the residual decoherence of a system, which is coupled to a general environment and to which a general dynamical decoupling is applied, is still missing. This is mostly due to the lack of a convenient tool. An unified framework to investigate these effects is thus much needed.

In this work we develop an unified numerical framework to simulate the renormalization of non-Markovian

dynamics of a system to which decoupling pulses are applied. It is capable of handling both unbounded and bounded pulses. It is also able to capture the effect of a general environment. Such a framework can help us to study the efficiency of a prescribed decoupling pulse in realistic situations. It might also open new avenues to optimize the decoupling pulses. To see what are the necessary ingredients of such a framework, recall that a quantum system without decoherence obeys Schrödinger equation, resulting a coherent, hence non-Markovian, dynamics. On the other hand, long time dynamics of an open quantum system in high temperature regime is typically Markovian[15]. A successful decoherence control should renormalize the dynamics, moving the system dynamics away from Markovian regime and move it into the non-Markovian regime. The residual decoherence, however, prevent us from simply using the Schrödinger equation to describe the renormalized dynamics. It is thus essential that such a framework can describe both the Markovian and non-Markovian dynamics for an open quantum system coupled to a general environment. Also, for numerical purpose a nonconvoluted master equation is highly desirable comparing to an integral-differential equation.

The nonconvoluted non-Markovian master equation [16, 17] derived from the non-Markovian quantum trajectories [18] formalism naturally provides such a framework. Markovian dynamics and Schrödinger dynamics can be seen as two limiting cases of the formalism. The formalism has been used to study the decoherence of the open quantum system in the non-Markovian regime [19, 20] as well as the non-Markovian dynamics of a two-level atom immersed in a photonic band-gap material[17]. In some cases the stochastic non-Markovian quantum trajectories can be formally averaged, resulting an exact non-Markovian master equation. In general, when the decoupling are applied to the system, an exact non-Markovian master equation cannot be formed[16]. But an approximated master equation can always be derived in the nearly Markovian limit[16] or weak coupling

limit[17]. It has been shown that the resulting non-Markovian master equation is valid in a wide range of parameter regime[16, 17]. It is this nonconvoluted master equation that will be taken as the starting point of our investigation of the renormalization of the non-Markovian dynamics.

The organization of the manuscript is as follows. In Section II we briefly review the non-Markovian quantum trajectory formalism and the resulting non-Markovian master equation. In section III we derive the non-Markovian master equations when the decoupling pulses are applied. In Section IV we simulate the renormalized dynamics after decoupling of a system which is driven by the Ornstein-Uhlenbeck noise while in Section V we study the renormalized dynamics of the spin-boson model. Three representative spectral densities are used. Bang-bang control pulses and continuous decoupling pulses are used in each case. The conclusion in Section VI briefly summarizes our findings.

II. NON-MARKOVIAN QUANTUM TRAJECTORIES AND MASTER EQUATIONS

The total Hamiltonian of our model of the open quantum system takes the form $H_{tot} = H_{sys} + H_{env} + H_{int}$, where $H_{sys} = H_0 + H_c(t)$ represents the system Hamiltonian which has been split into the original Hamiltonian H_0 and the dynamical decoupling control Hamiltonian H_c . $H_{env} = \sum_{\lambda} \omega_{\lambda} a_{\lambda}^{\dagger} a_{\lambda}$ represents the bosonic Hamiltonian of the environment and $H_{int} = \left(\sum_{\lambda} L g_{\lambda}^* a_{\lambda}^{\dagger} + L^{\dagger} g_{\lambda} a_{\lambda} \right)$ represents the interaction between system and environment. In our simulations we have set $H_0 = 0$ since we mainly focus on quantum memory In this work.

It has been shown that one can derive linear stochastic equations governing the dynamics of the system under the influence of the environment [18]. The stochastic Schrödinger equation can be obtained by expressing the total state $|\Psi(t)\rangle$ in terms of the Bargmann coherent state of the environment

$$|\Psi(t)\rangle = \int \frac{d^2 z}{\pi} e^{-|z|^2} |\psi(z^*, t)\rangle |z\rangle, \quad (1)$$

where $|z_{\lambda}\rangle \equiv \exp(z_{\lambda} a_{\lambda}^{\dagger})|0\rangle$ and $|z\rangle = |z_1\rangle|z_2\rangle \cdots |z_{\lambda}\rangle \cdots$. The resulting equation of $|\psi(z^*, t)\rangle$ reads

$$\begin{aligned} \frac{d}{dt} |\psi(z^*, t)\rangle &= [-iH_{sys} + L\eta^*(t)] |\psi(z^*, t)\rangle \\ &- L^{\dagger} \int_0^t ds \alpha(t, s) \frac{\delta |\psi(z^*, t)\rangle}{\delta \eta^*(s)}, \end{aligned} \quad (2)$$

where $\eta^*(t) = -i \sum_{\lambda} g_{\lambda}^* z_{\lambda}^* e^{i\omega_{\lambda} t}$ and

$$\alpha(t, s) = \sum_{\lambda} |g_{\lambda}|^2 e^{-i\omega_{\lambda}(t-s)} = \int_0^{\infty} d\omega J(\omega) e^{-i\omega(t-s)}. \quad (3)$$

Using this representation the reduced density matrix of the system can be expressed as

$$\rho(t) = \int \frac{d^2 z}{\pi} e^{-|z|^2} |\psi(z^*, t)\rangle \langle \psi(z^*, t)|. \quad (4)$$

If one choose to use Monte-Carlo integration to evaluate this expression, taking over the Gaussian distribution

$$\mathcal{M}[\dots] = \int \frac{d^2 z}{\pi} [\dots] \quad (5)$$

of z -vectors, then $\eta^*(t)$ can be interpreted as stochastic variables with following statistical properties

$$\mathcal{M}[\eta(t)] = \mathcal{M}[\eta(t)\eta(s)] = 0; \quad (6)$$

$$\mathcal{M}[\eta(t)\eta^*(s)] = \alpha(t, s). \quad (7)$$

Under this interpretation, Eq.(2) becomes a stochastic Schrödinger equation on the system. However it is still difficult to treat Eq.(2) due the the functional derivative with respect to the noise $\eta^*(s)$ under the memory integral. A nonconvoluted stochastic equation can be obtained by proposing the Ansatz

$$\frac{\delta |\psi(z^*, t)\rangle}{\delta \eta^*(s)} = O(t, s, \eta(t)) |\psi(z^*, t)\rangle, \quad (8)$$

where $O(t, s, \eta(t))$ is a linear operator that has to be determined for each case. With this replacement the stochastic equation becomes

$$\frac{d}{dt} |\psi(z^*, t)\rangle = [-iH_{sys} + L\eta^*(t) - L^{\dagger} \bar{O}(t, \eta^*)] |\psi(z^*, t)\rangle, \quad (9)$$

where $\bar{O}(t, \eta^*) = \int_0^t ds \alpha(t, s) O(t, s, \eta^*)$. For some cases it is possible to construct exactly the O operator. When it is difficult to identify the O operator, it is still possible to derive an approximate O operator by perturbation in terms of the coupling parameter [17] or the environmental correlation time[16], If the exact or approximate O operator is independent of the noise η^* , a master equation can be easily derived and takes the form:

$$\frac{d\rho(t)}{dt} = -i[H_{sys}, \rho] + [L, \rho(t)\bar{O}^{\dagger}(t)] + [\bar{O}(t)\rho(t), L^{\dagger}]. \quad (10)$$

Since we are interested in the renormalization of the non-Markovian dynamics we take the weak coupling limit in stead of the nearly Markovian limit. In this limit

$$O(t, s, \eta^*) \approx U(t-s) L U^{\dagger}(t-s), \quad (11)$$

where

$$U(t) = \mathcal{T} e^{-i \int_0^t du H_{sys}(u)}. \quad (12)$$

Hence

$$\bar{O}(t) = \int_0^t ds \alpha(t, s) U(t-s) L U^{\dagger}(t-s). \quad (13)$$

In the interaction picture with respect to the system Hamiltonian $\tilde{\rho}(t) = U^\dagger(t)\rho(t)U(t)$, the master equation becomes

$$\begin{aligned} \frac{d\tilde{\rho}(t)}{dt} &= \left[\tilde{L}(t), \tilde{\rho}(t) \int_0^t ds \alpha^*(t, s) \tilde{L}^\dagger(s) \right] \\ &+ \left[\int_0^t ds \alpha(t, s) \tilde{L}(s) \tilde{\rho}(t), \tilde{L}^\dagger(t) \right], \end{aligned} \quad (14)$$

where $\tilde{L}(t) = U^\dagger(t)LU(t)$. Note that when $\alpha(t, s) \rightarrow \delta(t-s)$ the master equation reduces to the standard Markovian Lindblad master equation in Heisenberg picture, i.e.

$$\frac{d\tilde{\rho}(t)}{dt} = [\tilde{L}(t), \tilde{\rho}(t)\tilde{L}^\dagger(t)] + [\tilde{L}(t)\tilde{\rho}(t), \tilde{L}^\dagger(t)]. \quad (15)$$

III. DYNAMICAL DECOUPLING

In the language of standard periodic dynamical decoupling one usually starts from the total Hamiltonian $H_{tot} = \sum_\gamma S_\gamma \otimes B_\gamma$. A periodic control Hamiltonian $H_c(t)$ with period T_c is introduced to decouple the system from the environment. Using Magnus expansion[21] the average Hamiltonian governing the stroboscopic dynamics has the form

$$\bar{H}_{tot} = \frac{1}{T_c} \int_0^{T_c} ds \left[U_c^\dagger(s) \sum_\gamma S_\gamma \otimes U_c(s) \right] B_\gamma. \quad (16)$$

A properly designed control Hamiltonian can generate an $U_c(t)$ which results in a zero \bar{H}_{tot} . Many methods have been developed to design the decoupling pulses [3, 4, 5, 6, 7, 8]. In this work we focus on investigating the renormalized dynamics when a decoupling pulses based on those methods are applied to the system. It should be noted, however, that it is also possible to design decoupling pulses based on Eq.(14). We sketch the procedure as follows. First decomposes L into $L = L_A + iL_B$ where both L_A and L_B are Hermitian. It is then easy to verify that the decoupling condition (for the case of quantum memory) is

$$\int_0^{T_c} ds \alpha(t, s) \tilde{L}_A(s) = \lambda_A, \quad \int_0^{T_c} ds \alpha(t, s) \tilde{L}_B(s) = \lambda_B, \quad (17)$$

where λ_A and λ_B are real numbers. When this condition is satisfied, the master equation turns into

$$\begin{aligned} \left. \frac{d\rho(t)}{dt} \right|_{t=T_c} &= [\tilde{L}_A + i\tilde{L}_B, \tilde{\rho}(t)(\lambda_A - i\lambda_B)] + h.c. \\ &= -i[(-2\lambda_A\tilde{L}_B), \tilde{\rho}(t)] - i[(+2\lambda_B\tilde{L}_A), \tilde{\rho}(t)] \\ &= -i[\tilde{H}_{eff}, \tilde{\rho}(t)], \end{aligned} \quad (18)$$

which contains no decoherence terms. The connection to the standard dynamical decoupling can be seen more transparently if one assumes that $\alpha(t, s) = \theta(|t-s|/T_c)/T_c$ and $H_0 = 0$. The decoupling conditions then becomes

$$\int_0^{T_c} ds U_c^\dagger(s) L_{A,B} U_c(s) = \lambda_{A,B}, \quad (19)$$

which is exactly the standard bang-bang decoupling condition[6].

In the following we will derive the non-Markovian master equations when continuous or bang-bang decoupling is applied to the system. Those master equations will be used in next two sections to simulate the renormalized dynamics. First consider the case where $L = \sigma_z$. Without the control Hamiltonian the master equation is

$$\begin{aligned} \frac{d\tilde{\rho}(t)}{dt} &= \left[\sigma_z, \tilde{\rho}(t) \int_0^t ds \alpha^*(t, s) \sigma_z \right] + h.c.. \\ &= \int_0^t ds \mu(t, s) \begin{bmatrix} 0 & -4\tilde{\rho}_{01} \\ -4\tilde{\rho}_{10} & 0 \end{bmatrix}, \end{aligned} \quad (20)$$

where we have decomposed $\alpha(t, s)$ into its real part $\mu(t, s)$ and imaginary part $\nu(t, s)$ but with the convention $\alpha = \mu - i\nu$. Note that $\nu(t, s)$ doesn't contribute the decoherence in this case. According to Ref.[6], a continuous decoupling can be achieved by using the control Hamiltonian $H_c(t) = a_x(t)\sigma_x$, where we have assumed $H_0 = 0$ since we are interested in the quantum memory. Under such a decoupling the master equation becomes

$$\frac{d\tilde{\rho}(t)}{dt} = \left[\sigma_z(t), \tilde{\rho}(t) \int_0^t ds \alpha^*(t, s) \sigma_z(s) \right] + h.c.. \quad (21)$$

To proceed, one needs to find the associated time evolution operator

$$U_c(t) = e^{-i \int_0^t du a_x(u) \sigma_x} = \begin{bmatrix} \cos(A(t)) & -i \sin(A(t)) \\ -i \sin(A(t)) & \cos(A(t)) \end{bmatrix}, \quad (22)$$

where $A(t) = \int_0^t du a_x(u)$, and

$$\sigma_z(s) = U_c^\dagger(s) \sigma_z U_c(s) = \begin{bmatrix} \cos(2A(s)) & -i \sin(2A(s)) \\ i \sin(2A(s)) & \cos(2A(s)) \end{bmatrix}. \quad (23)$$

It has been shown in Ref.[6] that decoupling condition can be achieved if $2A(T_c/2) = \pi$ and $2A(T_c/2 + s) = \pi + 2A(s)$. Under this condition one has

$$\begin{aligned}
\int_0^{T_c} dt U_c^\dagger(s) \sigma_z U_c(s) &= \int_0^{\frac{T_c}{2}} dt \begin{bmatrix} \cos(2A(s)) + \cos(2A(\frac{T_c}{2} + s)) & -i \sin(2A(s)) - i \sin(2A(\frac{T_c}{2} + s)) \\ i \sin(2A(s)) + i \sin(2A(\frac{T_c}{2} + s)) & \cos(2A(s)) + \cos(2A(\frac{T_c}{2} + s)) \end{bmatrix} \\
&= \int_0^{\frac{T_c}{2}} dt \begin{bmatrix} \cos(2A(s)) - \cos(2A(s)) & -i \sin(2A(s)) + i \sin(2A(s)) \\ i \sin(2A(s)) - i \sin(2A(s)) & \cos(2A(s)) - \cos(2A(s)) \end{bmatrix} = 0. \quad (24)
\end{aligned}$$

Hence at the ideal limit where $T_c \rightarrow 0$ the decoherence is totally suppressed, i.e.,

$$\lim_{T_c \rightarrow 0, N \rightarrow \infty, t = NT_c} \left. \frac{d\tilde{\rho}(t)}{dt} \right|_{t=NT_c} = 0. \quad (25)$$

However when T_c is finite, the decoupling cannot be perfectly achieved. The error associated with finite T_c will depend on the correlation function $\alpha(t, s)$ and the envelope function $a_x(t)$. The master equation associate with a finite T_c can be easily derived. After some algebra we find

$$\begin{aligned}
\frac{d\tilde{\rho}}{dt} &= 2 \sin(2A(t)) \int_0^t ds \mu(t, s) \sin(2A(s)) \\
&\times \begin{bmatrix} \tilde{\rho}_{11}(t) - \tilde{\rho}_{00}(t) & -\tilde{\rho}_{01}(t) - \tilde{\rho}_{10}(t) \\ -\tilde{\rho}_{01}(t) - \tilde{\rho}_{10}(t) & -\tilde{\rho}_{11}(t) + \tilde{\rho}_{00}(t) \end{bmatrix} \\
&+ 2 \sin(2A(t)) \int_0^t ds \nu(t, s) \cos(2A(s)) \\
&\times \begin{bmatrix} \tilde{\rho}_{01}(t) + \tilde{\rho}_{10}(t) & -\tilde{\rho}_{00}(t) + \tilde{\rho}_{11}(t) \\ -\tilde{\rho}_{00}(t) + \tilde{\rho}_{11}(t) & -\tilde{\rho}_{01}(t) - \tilde{\rho}_{10}(t) \end{bmatrix}, \quad (26)
\end{aligned}$$

where we have used $\alpha(t, s) = \mu(t, s) - i\nu(t, s)$. Once the envelop function $a_x(t)$ is identified, this equation can be used to calculate the renormalized dynamics. Note that under continuous decoupling both μ and ν contribute to the decoherence.

On the other hand for bang-bang control the function $A(t)$ takes the special form

$$A(t) = \frac{\pi}{2} \sum_{i=0}^{N-1} \Theta(t - i\frac{T_c}{2}). \quad (27)$$

It is then straightforward to show that $\sigma_z(s) = f(s)\sigma_z$ where $f(s) = +1$ for $s \in (2i\frac{T_c}{2}, 2i + 1\frac{T_c}{2})$ and $f(s) = -1$ for $s \in (2i + 1\frac{T_c}{2}, 2i + 2\frac{T_c}{2})$, $i = 1, 2, \dots, [\frac{t}{T_c}]$. The resulting master equation is

$$\frac{d\tilde{\rho}(t)}{dt} = \int_0^t ds \mu(t, s) f(s) \begin{bmatrix} 0 & -4\tilde{\rho}_{01} \\ -4\tilde{\rho}_{10} & 0 \end{bmatrix}. \quad (28)$$

In other words, applying bang-bang control results in the renormalization of the function $\mu(t, s)$. The renormalized $\mu(t, s)$ can be evaluated numerically as follows

$$\begin{aligned}
&\int_0^t ds \mu(t, s) f(s) \quad (29) \\
&= \sum_{k=1}^{2N} \int_{(k-1)\frac{T_c}{2}}^{k\frac{T_c}{2}} ds \mu(t, s) (-1)^{k-1} \sigma_z + \int_{NT_c}^t ds \mu(t, s) \sigma_z.
\end{aligned}$$

We observe that the master equation under bang-bang control takes a simpler form compared to the one under continuous decoupling. This suggests that there might be some dynamical effects which cannot be captured if one only studies the ideal bang-bang limit.

Consider next the case where $L = \sigma_-$. Without the control Hamiltonian the master equation is

$$\begin{aligned}
\frac{d\tilde{\rho}(t)}{dt} &= \left[\sigma_-, \tilde{\rho}(t) \int_0^t ds \alpha^*(t, s) \sigma_+ \right] + h.c.. \\
&= \int_0^t ds \mu(t, s) \begin{bmatrix} 2\tilde{\rho}_{11}(t) & -\tilde{\rho}_{01} \\ -\tilde{\rho}_{10} & -2\tilde{\rho}_{11}(t) \end{bmatrix} \\
&+ \int_0^t ds \nu(t, s) \begin{bmatrix} 0 & -i\tilde{\rho}_{01} \\ +i\tilde{\rho}_{10} & 0 \end{bmatrix}. \quad (30)
\end{aligned}$$

Note that in this case both μ and ν contribute to the decoherence. When continuous decoupling is applied the master equation becomes

$$\begin{aligned}
&\frac{d\rho}{dt} \quad (31) \\
&= \begin{bmatrix} -(\tilde{\mu}(t) + \tilde{\mu}^*(t))\tilde{\rho}_{00}(t) & -\tilde{\mu}^*(t)\tilde{\rho}_{01}(t) \\ -\tilde{\mu}(t)\tilde{\rho}_{10}(t) & -(\tilde{\mu}(t) + \tilde{\mu}^*(t))\tilde{\rho}_{00}(t) \end{bmatrix} \\
&+ \begin{bmatrix} (-i\tilde{\nu}(t) + i\tilde{\nu}^*(t))\tilde{\rho}_{00}(t) & i\tilde{\nu}^*(t)\tilde{\rho}_{01}(t) \\ -i\tilde{\nu}(t)\tilde{\rho}_{10}(t) & (+i\tilde{\nu}(t) - i\tilde{\nu}^*(t))\tilde{\rho}_{00}(t) \end{bmatrix},
\end{aligned}$$

where

$$\tilde{\mu}(t) = 4e^{-i2A(t)} \int_0^t ds \mu(t, s) e^{i2A(s)}, \quad (32)$$

and

$$\tilde{\nu}(t) = 4e^{-i2A(t)} \int_0^t ds \nu(t, s) e^{i2A(s)}. \quad (33)$$

While when bang-bang control is applied, the master equation becomes

$$\begin{aligned}
\frac{d\tilde{\rho}(t)}{dt} &= \int_0^t ds \mu(t, s) f(s) \begin{bmatrix} 2\tilde{\rho}_{11}(t) & -\tilde{\rho}_{01} \\ -\tilde{\rho}_{10} & -2\tilde{\rho}_{11}(t) \end{bmatrix} \\
&+ \int_0^t ds \nu(t, s) f(s) \begin{bmatrix} 0 & -i\tilde{\rho}_{01} \\ +i\tilde{\rho}_{10} & 0 \end{bmatrix}. \quad (34)
\end{aligned}$$

In contrast to the case where $L = \sigma_z$, in this case both μ and ν contribute to the decoherence.

IV. ORNSTEIN-UHLENBECK NOISE

In this section we study how the dynamics of a system driven by the Ornstein-Uhlenbeck noise is renormalized by the bang-bang and continuous decoupling pulses. The Ornstein-Uhlenbeck noise is characterized by the exponential correlation function

$$\alpha(t, s) = \mu(t, s) = \frac{1}{2\tau} e^{-\frac{|t-s|}{\tau}}. \quad (35)$$

This particular form of the correlation function enables us to carry out analytically most of the calculation. The main purpose is to illustrate how the decoherence is renormalized by the bang-bang or continuous decoupling pulses. First consider the case where $L = \sigma_z$. Using the result in proceeding section, we find that without the control Hamiltonian the off-diagonal term of the density matrix decays as follows:

$$\frac{d\tilde{\rho}_{01}}{dt} = -2 \left(1 - e^{-t/\tau}\right) \tilde{\rho}_{01}. \quad (36)$$

When a control Hamiltonian of the form $H_c(t) = a_x(t)\sigma_x$ is applied and the resulting $A(t)$ has the form $A(t) = \pi t/T_c$, the renormalized master equation becomes

$$\begin{aligned} \frac{d\tilde{\rho}(t)}{dt} &= \frac{2M_s(t) \sin(2\pi t/T_c)}{\left(1 + (2\pi\tau/T_c)^2\right)} \\ &\times \begin{bmatrix} \tilde{\rho}_{11}(t) - \tilde{\rho}_{00}(t) & -\tilde{\rho}_{01}(t) - \tilde{\rho}_{10}(t) \\ -\tilde{\rho}_{01}(t) - \tilde{\rho}_{10}(t) & -\tilde{\rho}_{11}(t) + \tilde{\rho}_{00}(t) \end{bmatrix}, \end{aligned} \quad (37)$$

where

$$M_s(t) = e^{-t/\tau} \left(\frac{2\pi\tau}{T_c}\right) - \frac{2\pi\tau}{T_c} \cos\left(\frac{2\pi t}{T_c}\right) + \sin\left(\frac{2\pi t}{T_c}\right). \quad (38)$$

It is important to observe that

$$\lim_{T_c \rightarrow 0, N \rightarrow \infty, t = NT_c} \frac{2M_s(t) \sin(2\pi t/T_c)}{\left(1 + (2\pi\tau/T_c)^2\right)} = 0. \quad (39)$$

If a different envelope function $a_x(t)$ is used, the resulting renormalized master equation will have a similar form, but a different time-dependent pre-factor will appear.

On the other hand, if bang-bang decoupling is applied the renormalized master equation becomes

$$\frac{d\tilde{\rho}_{01}}{dt} = -2e^{-\frac{t}{\tau}} \left(e^{\frac{t}{\tau}} - 1 + 2e^{\frac{T_c}{2\tau}} \frac{1 - e^{\frac{NT_c}{\tau}}}{1 + e^{\frac{T_c}{\tau}}} \right) \tilde{\rho}_{01}. \quad (40)$$

Note again that

$$\lim_{T_c \rightarrow 0, N \rightarrow \infty, t = NT_c} \frac{1}{2} e^{-\frac{t}{\tau}} \left(e^{\frac{t}{\tau}} - 1 + 2e^{\frac{T_c}{2\tau}} \frac{1 - e^{\frac{NT_c}{\tau}}}{1 + e^{\frac{T_c}{\tau}}} \right) = 0. \quad (41)$$

Consider next the case where $L = \sigma_+$. In this case the master equation without the control is

$$\frac{d\tilde{\rho}}{dt} = \frac{1}{2}(1 - e^{-t/\tau}) \begin{bmatrix} 2\tilde{\rho}_{11}(t) & -2\tilde{\rho}_{01}(t) \\ -2\tilde{\rho}_{01}(t) & -2\tilde{\rho}_{11}(t) \end{bmatrix}. \quad (42)$$

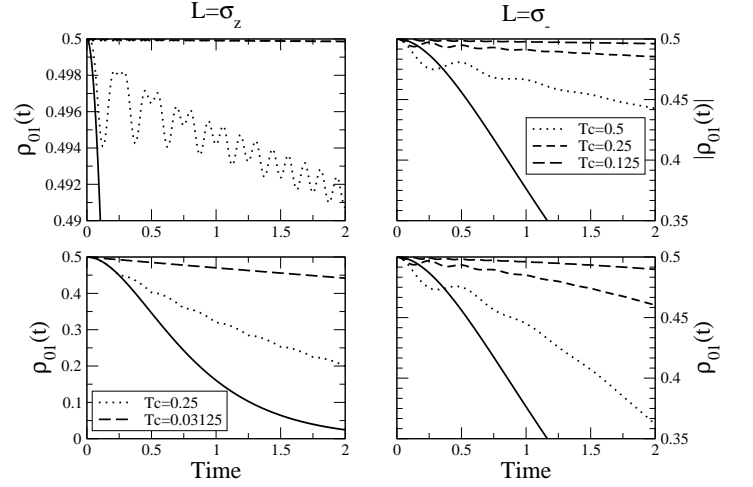


FIG. 1: Time evolution of $\rho_{01}(t)$ for a system driven by the Ornstein-Uhlenbeck noise and bang-bang or continuous control. In all figures we set $\tau = 0.5$. Upper-left: $L = \sigma_z$ and bang-bang control is applied. Bottom-left: $L = \sigma_z$ and continuous control is applied. Right: $L = \sigma_z$ and continuous control is applied. In this case $\rho_{01}(t)$ is complex and its absolute value and real part are plotted respectively.

When the control Hamiltonian $H_c(t) = a_z(t)\sigma_z$ is applied and $A(t) = \pi t/T_c$, the renormalized master equation is

$$\begin{aligned} \frac{d\tilde{\rho}(t)}{dt} & \\ &= \begin{bmatrix} -(\tilde{\mu}(t) + \tilde{\mu}^*(t)\rho_{00}(t)) & -\tilde{\mu}^*(t)\rho_{01}(t) \\ -\tilde{\mu}(t)\rho_{10}(t) & (\tilde{\mu}(t) + \tilde{\mu}^*(t)\rho_{00}(t)) \end{bmatrix}, \end{aligned} \quad (43)$$

where

$$\tilde{\mu}(t) = 2 \frac{1 - e^{-t/\tau} e^{-i2\pi t/T_c}}{1 + i2\pi\tau/T_c}. \quad (44)$$

While when bang-bang control is applied, the resulting master equation is

$$\begin{aligned} \frac{d\tilde{\rho}(t)}{dt} &= -\frac{1}{2} e^{-\frac{t}{\tau}} \left(e^{\frac{t}{\tau}} - 1 + 2e^{\frac{T_c}{2\tau}} \frac{1 - e^{\frac{NT_c}{\tau}}}{1 + e^{\frac{T_c}{\tau}}} \right) \\ &\times \begin{bmatrix} 2\tilde{\rho}_{11}(t) & -\tilde{\rho}_{01}(t) \\ -\tilde{\rho}_{10}(t) & -2\tilde{\rho}_{11}(t) \end{bmatrix}. \end{aligned} \quad (45)$$

It is instructive to simulate numerically the time evolution of $\rho_{01}(t)$ under bang-bang and continuous decoupling. We assume that initially the system is at pure state $|\psi\rangle = \frac{1}{\sqrt{2}}(|0\rangle + |1\rangle)$. In Fig.1 (left) we plot $\rho_{01}(t)$ as function of time for the case where $L = \sigma_z$. The renormalized dynamics under bang-bang control and continuous decoupling are plotted respectively. In this case $\rho_{01}(t)$ is always real. In Fig.1 (right) we plot the real part and the absolute value of $\rho_{01}(t)$ for the case where $L = \sigma_-$. We only plot the renormalized dynamics under continuous decoupling since the dynamics under bang-bang control is identical to the case where $L = \sigma_z$ with a different overall constant.

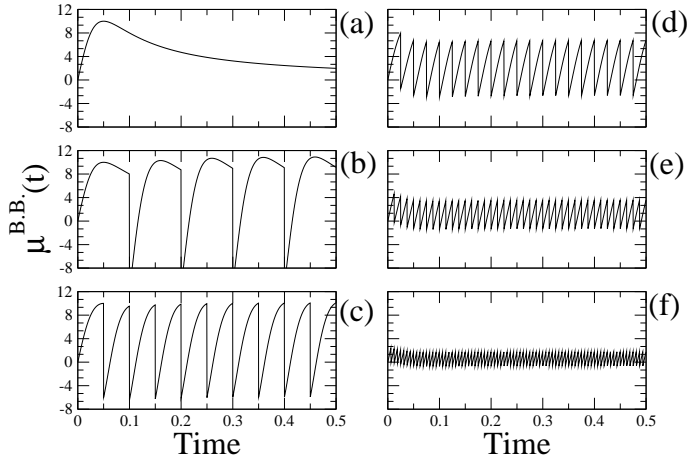


FIG. 2: $\mu_1^{B.B.}(t)$ as a function of time with an Ohmic environment and $\Lambda = 20$. (a) Without bang-bang control. (b) $T_c = 0.5$. (c) $T_c = 0.25$. (d) $T_c = 0.125$. (e) $T_c = 0.0625$.

It is evident that when bang-bang or continuous decoupling is applied the decoherence is suppressed and better result is achieved for shorter T_c . It is important to note that the efficiency for those two class of decoupling is different. Continuous decoupling results in a much better suppression. The continuous decoupling can already suppress the decay of $\tilde{\rho}_{01}$ when $T_c \sim \tau$. Although we only show one particular realization of the continuous pulse, numerical evidence shows that continuous pulse always results in better suppression for this noise model. Further optimization on pulse shape is possible and worth more investigation. It should also be noted that that σ_z and σ_- coupling to the environment results in quantitatively different renormalized dynamics.

V. SPIN-BOSON MODEL

In this section we turn our attention to the spin-boson model. It is known that the zero temperature correlation function of bosonic environment can be written as

$$\alpha(t, s) = \int_0^\infty d\omega J(\omega) [\cos(\omega(t-s)) - i \sin(\omega(t-s))], \quad (46)$$

where the spectral density $J(\omega)$ has the form

$$J(\omega) = \omega^p e^{-\omega/\Lambda_U V}. \quad (47)$$

When $p = 1$ it corresponds to the Ohmic environment, when $p > 1$ it corresponds to the supra-Ohmic environment, and when $p < 1$ it corresponds to the sub-Ohmic environment. For $1/f$ type sub-Ohmic environment, i.e., $p = -1$, an infrared cutoff Λ_{IR} is also necessary.

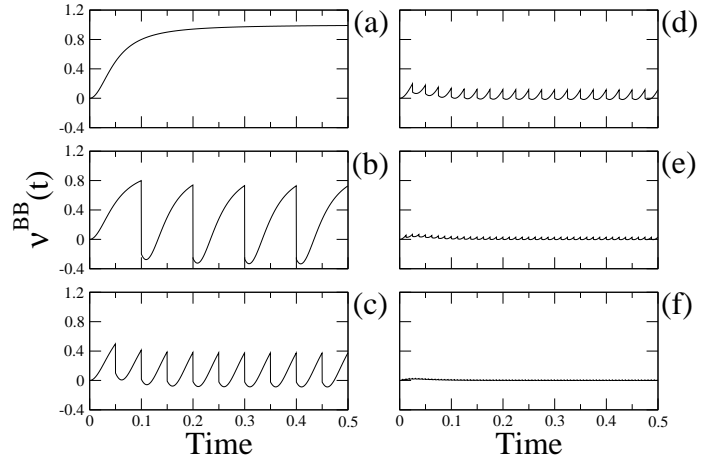


FIG. 3: $\nu_1^{B.B.}(t)$ as a function of time with an Ohmic environment and $\Lambda = 20$. (a) Without bang-bang control. (b) $T_c = 0.5$. (c) $T_c = 0.25$. (d) $T_c = 0.125$. (e) $T_c = 0.0625$.

A. Ohmic and Supra-Ohmic

Consider first the Ohmic and supra-Ohmic environment. It is instructive to exam how μ and ν are renormalized by the bang-bang control. In Fig.2 we plot $\mu^{B.B.}(t) \equiv \int_0^t ds \mu(t, s) f(s)$ for an Ohmic environment. It is clear from the figure that when T_c is not small enough, $\mu^{B.B.}(t)$ might be larger than the original $\mu(t)$ in some temporal regime, which is undesirable. For small enough T_c the $\mu(t)$ is always suppressed. In Fig.3 we plot $\nu^{B.B.} \equiv \int_0^t ds \nu(t, s) f(s)$ for the same system. We find that $\nu(t)$ is always suppressed by the bang-bang control. Continuous decoupling, on the other hand, will mix the real and imaginary part of $\alpha(t, s)$. In some cases this will deteriorate the efficiency of the decoupling. In the following we present the numerical results for various scenarios.

1. $L = \sigma_z$, bang-bang decoupling

When $L = \sigma_z$ the master equation at zero temperature without the control Hamiltonian is reduced to

$$\frac{d\tilde{\rho}_{01}(t)}{dt} = -4 \int_0^t ds \mu_{p,\Lambda}(t-s) \tilde{\rho}_{01}(t), \quad (48)$$

where

$$\mu_{p,\Lambda}(t-s) = \int_0^\infty d\omega \omega^p e^{-\omega/\Lambda} \cos(\omega(t-s)). \quad (49)$$

When bang-bang control is applied the master equation reads

$$\frac{d\tilde{\rho}_{01}(t)}{dt} = -4 \int_0^t ds \mu_{p,\Lambda}(t-s) f(s) \tilde{\rho}_{01}(t), \quad (50)$$

We define $T_2(\Lambda)$ to be the time which satisfies the condition $\tilde{\rho}_{01}(T_2) = e^{-1} \tilde{\rho}_{01}(0)$. In the Markovian limit this

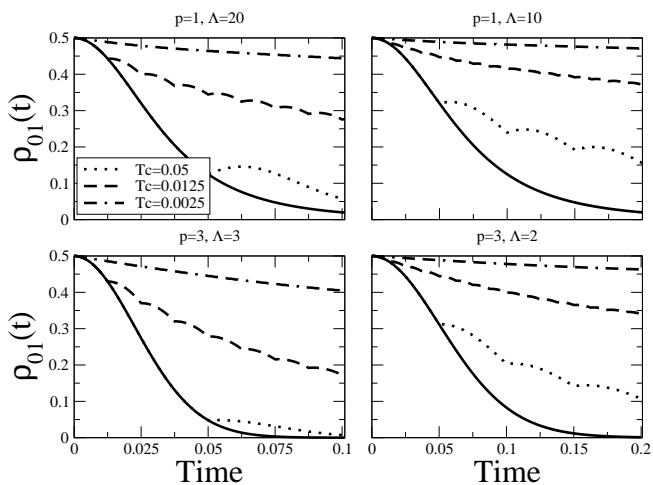


FIG. 4: $\tilde{\rho}_{01}(t)$ under bang-bang control for a system coupled to an Ohmic ($p = 1$) and Supra-Ohmic ($p = 3$) environment and $L = \sigma_z$. Solid line represents the free decay without bang-bang control.

definition will coincide with the typical definition of T_2 . In Fig.4 we plot the time evolution of $\rho_{01}(t)$ under bang-bang control for a system coupled to an Ohmic ($p = 1$) and a supra-Ohmic ($p = 3$) environment. We have picked two different cut-offs Λ for each environment. It is evident that the free decay is not a simple exponential and the detail functional form of the decay depends on p and Λ . Since the decay is non-exponential, there is no single time scale to which T_c can be compared. Roughly speaking, however, one can still say that the decoupling is efficient when T_c is smaller than $T_2(p, \Lambda)$.

2. $L = \sigma_z$, continuous decoupling

When continuous decoupling is applied the differential equation for $\tilde{\rho}_{01}(t)$ reads,

$$\frac{d\tilde{\rho}_{01}(t)}{dt} = -2 \sin\left(\frac{2\pi t}{T_c}\right) \int_0^t ds \mu_{p,\Lambda}(t-s) \sin\left(\frac{2\pi s}{T_c}\right) \tilde{\rho}_{01}, \quad (51)$$

where we have assumed the same initial condition and $A(t) = \pi t/T_c$. Note that in this case $\tilde{\rho}_{01}(t)$ remains real during the evolution. In Fig.5 we plot the time evolution of $\tilde{\rho}_{01}(t)$ under continuous decoupling control for a system coupled to an Ohmic ($p = 1$) and a supra-Ohmic ($p = 3$) environment. Similar to the case where the system is driven by the Ornstein-Uhlenbeck noise, continuous decoupling is more efficient for the same T_c .

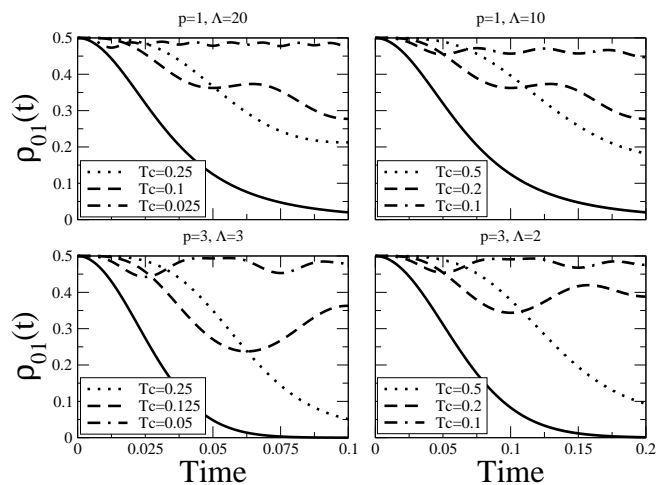


FIG. 5: $\tilde{\rho}_{01}(t)$ under continuous decoupling for a system coupled to an Ohmic ($p = 1$) and Supra-Ohmic ($p = 3$) environment and $L = \sigma_z$. Solid line represents the free decay without decoupling control.

3. $L = \sigma_-$, bang-bang decoupling

Consider next the case where $L = \sigma_-$. Without the decoupling pulse the differential equation for $\tilde{\rho}_{01}(t)$ reads

$$\frac{d\tilde{\rho}_{01}(t)}{dt} = - \int_0^t ds (\mu_{p,\Lambda}(t,s) + i\nu_{p,\Lambda}(t,s)) \tilde{\rho}_{01}(t), \quad (52)$$

while when bang-bang control is applied, it becomes

$$\frac{d\tilde{\rho}_{01}(t)}{dt} = - \int_0^t ds (\mu_{p,\Lambda}(t,s) + i\nu_{p,\Lambda}(t,s)) f(s) \tilde{\rho}_{01}(t), \quad (53)$$

In contrast to the case where $L = \sigma_z$, it is now necessary to evaluate the renormalization of both μ and ν . In Fig.6 (Fig.7) we plot the renormalized dynamics of $\tilde{\rho}_{01}(t)$ under bang-bang control for a system coupled to an Ohmic (supra-Ohmic) environment. The behavior of the real part of $\tilde{\rho}_{01}(t)$ is qualitatively similar to the case where $L = \sigma_z$. The imaginary part, on the other hand, deviates from zero as time goes. In most cases it grows monotonically. In some cases, however, it shows quasi-oscillation behavior when no decoupling pulse is applied. For some range of the T_c , the bang-bang control cannot efficiently suppress the growth of the imaginary part. For small enough T_c , the renormalized dynamics of the imaginary part resumes its monotonic increase, with a suppressed increase rate. It should be noted that the overall efficiency is qualitatively similar to the case where $L = \sigma_z$ since the decay of the real part of $\tilde{\rho}_{01}$ dominates the decoherence.

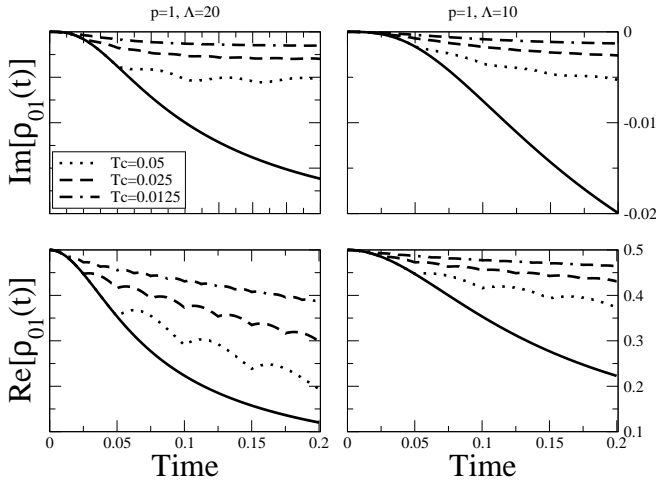


FIG. 6: $\tilde{\rho}_{01}(t)$ under bang-bang control for a system coupled to an Ohmic ($p = 1$) environment and $L = \sigma_-$. Solid line

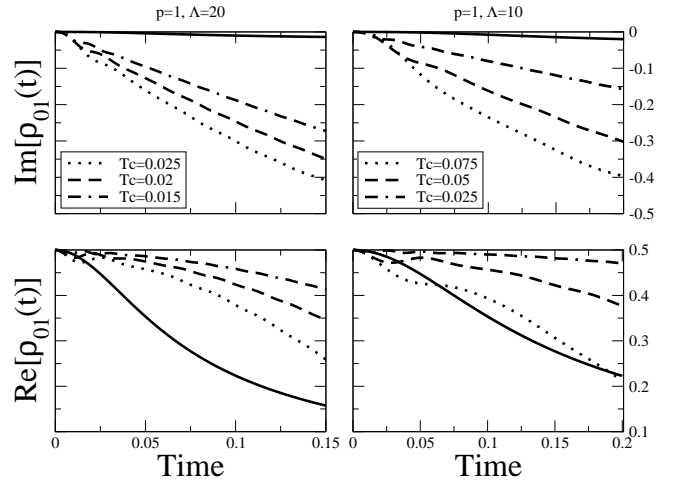


FIG. 8: $\tilde{\rho}_{01}(t)$ under continuous control for a system coupled to an Ohmic ($p = 1$) environment and $L = \sigma_-$. Solid line represents the free decay without bang-bang control.

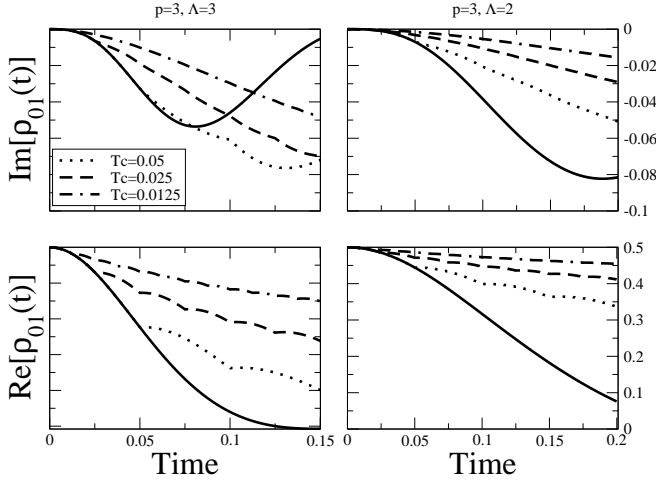


FIG. 7: $\tilde{\rho}_{01}(t)$ under bang-bang control for a system coupled to a Super-Ohmic ($p = 3$) environment and $L = \sigma_-$. Solid line represents the free decay without bang-bang control.

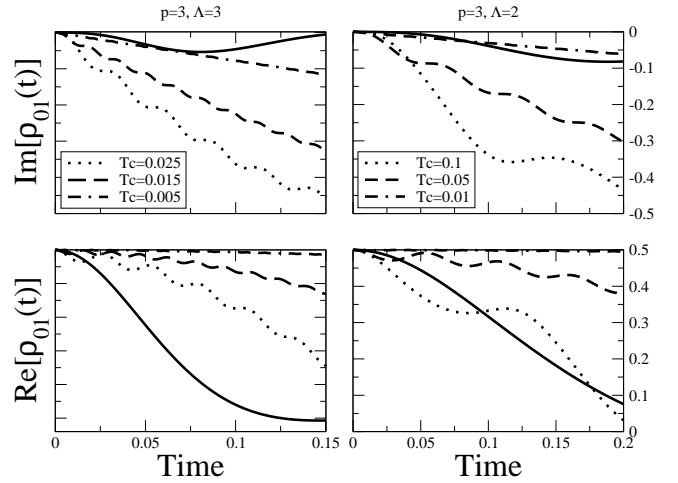


FIG. 9: $\tilde{\rho}_{01}(t)$ under continuous control for a system coupled to a Super-Ohmic ($p = 3$) environment and $L = \sigma_-$. Solid line represents the free decay without bang-bang control.

4. $L = \sigma_-$, continuous decoupling

When continuous decoupling is applied the differential equation for $\tilde{\rho}_{01}(t)$ reads,

$$\frac{d\tilde{\rho}_{01}(t)}{dt} = 4e^{-2iA(t)} \int_0^t ds (\tilde{\mu}_{p,\Lambda}(t) - i\tilde{\nu}_{p,\Lambda}(t)) e^{2iA(s)} \tilde{\rho}_{01}. \quad (54)$$

In Fig.8 (Fig.9) we plot the renormalized dynamics of $\tilde{\rho}_{01}(t)$ under continuous control for a system coupled to an Ohmic (supra-Ohmic) environment. The salient feature to be observed is the dynamics of the imaginary part of $\tilde{\rho}_{01}(t)$. It only increases slowly for the case of free decay. When the continuous decoupling is turned on, however, the imaginary part grows much more rapidly. This behavior results in the deterioration of the efficiency. The growth of the imaginary part can be suppressed by de-

creasing the T_c . But a very small T_c is needed to suppress the imaginary part to the same level as the one in free decay. This feature is due to the fact that when continuous decoupling is turned on, μ and ν are not separately renormalized. The decoupling pulse will mix μ and ν , resulting a more rapid growth of the imaginary part.

B. Sub-Ohmic

Now turn our attention to the sub-Ohmic environment. We will focus on the $1/f$ type environment. For $1/f$ type sub-Ohmic environment the correlation function takes the form

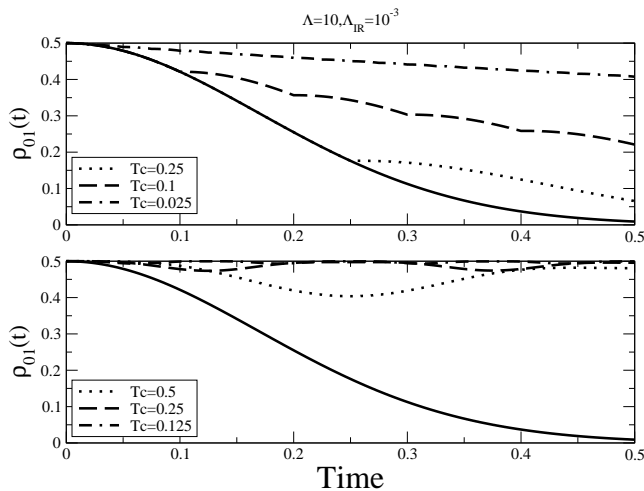


FIG. 10: $\tilde{\rho}_{01}(t)$ under bang-bang (upper half) or continuous (bottom half) control for a system coupled to an $1/f$ -noise environment and $L = \sigma_z$. Solid line represents the free decay without decoupling control.

$$\alpha(t, s) = \int_{\Lambda_{IR}}^{\infty} d\omega \frac{e^{-\frac{\omega}{\Lambda_{UV}}}}{\omega} [\cos(\omega(t-s)) - i \sin(\omega(t-s))], \quad (55)$$

where an infrared cutoff is introduced to ensure the convergence. In Fig.10 we plot the renormalized dynamics of $\tilde{\rho}_{01}(t)$ for a system with $L = \sigma_z$ under bang-bang or continuous decoupling. We observe that continuous decoupling is more efficient. In Fig.11 we plot the renormalized dynamics of $\tilde{\rho}_{01}(t)$ for a system with $L = \sigma_-$ under bang-bang or continuous decoupling. In this case we observe that imaginary begins to grow rapidly once the continuous decoupling is turned on. This is again due to the mixing of $\mu(t)$ and $\nu(t)$ via the continuous decoupling. In this scenario the bang-bang control is more efficient.

VI. SUMMARY AND DISCUSSION

In summary we have developed a numerical framework to investigate the renormalization of the non-Markovian dynamics due to the dynamical decoupling pulses. The nonconvoluted non-Markovian master equation used in this work is derived from the non-Markovian quantum trajectories formalism. The resulting master equation is written in a convenient form such that once the decoupling pulses are prescribed, the renormalized dynamic can be readily simulated. In order to validate the framework we have performed a comprehensive simulation of the renormalized dynamics under following scenarios. We have investigated two different system-environment interactions, namely $L = \sigma_z$ and $L = \sigma_-$. Three representative environmental spectral densities are used, including supra-Ohmic, Ohmic, and sub-Ohmic environment. Two

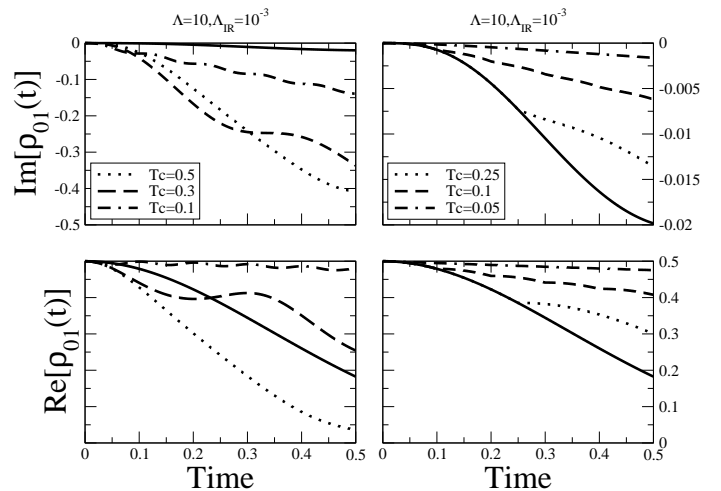


FIG. 11: $\tilde{\rho}_{01}(t)$ under bang-bang (right two) or continuous (left two) control for a system coupled to an $1/f$ -noise environment and $L = \sigma_-$. Solid line represents the free decay without decoupling control.

kinds of decoupling pulses are considered. One is the typical bang-bang decoupling while the other one is the continuous decoupling. Note also that the period of the decoupling cycle, T_c , is finite in all of the simulations.

The numerical results presented in Section IV and V clearly demonstrate that the framework is capable of simulate the renormalization of the dynamics of a system coupled to a general environment under the action of a general decoupling pulse. The renormalized dynamics, in turn, determined the true efficiency of a decoupling pulse. We observe that different decoupling pulses sometimes give rise to qualitatively different renormalized dynamics, and the difference depends on both the system-environment interaction and the environmental correlation function. Recall that, however, these decoupling pulses are designed solely based on the form of the system-environment interaction, and they all attain the desired decoupling in the ideal limit. To better understand the implication of this observation one should notice that bang-bang decoupling can be viewed as an unphysical limit of the continuous decoupling[6]. Within the framework presented in this work, bang-bang decoupling simply corresponds to a very special envelop function. On the other hand, only one particular envelop function $A(t)$ is used for continuous decoupling in this work. In other words, two special envelope function are chosen to carry out the simulations throughout this work. In reality the real envelop function of the pulse, which might be designed based on other methods, should fall somewhere in between these two limiting cases. The profound difference in the renormalized dynamics observed in this work thus indicates that the real efficiency depends crucially on the actual shape of the envelop function, the spectral density of the environment, and the nature of the system-environment interaction. For example, our results show that continuous decoupling is more ad-

vantageous in many cases, as can be seen in Fig.1, Fig.4, Fig.5, and Fig.10. However when $L = \sigma_-$ the continuous decoupling will induce mixing between the real and imaginary part of the environment correlation function, making the decoupling less efficient. Above observation actually leads to the possibility of further optimizing the decoupling pulses basing on the master equation Eq (14) and using techniques such as pulse shaping[22].

The framework developed here can server multiple purposes. The primary goal is to server as a convenient tool in investigating the efficiency of a prescribed decoupling pulse. Although we have only shown the cases where the deterministic, periodic pulses are applied. The framework can also easily simulate the renormalized dynamics induced by a random decoupling [5, 6] or a concatenated dynamical decoupling[10, 23]. It can also be used as an alternative starting point to design the decoupling pulse. One can naturally view the non-Markovian master equation under decoupling as a dynamical map, whose convergence the ideal fixed point of zero system-environment interaction can be studied. The framework is not limited

to a single two-level system coupled to a general environment. It is also suitable for studying the renormalized dynamics of a multi-level system. Such a multi-level system can represent a multi physical or logical qubit system. When necessary, one can unravel the master equation and use the corresponding stochastic Schrödinger equation, which is numerically advantageous for a large system. It is also important to note that if eventually a continuous measurement interpretation of non-Markovian stochastic equations is developed, this framework can be adapted to study the error correction and feedback control in the non-Markovian regime.

Acknowledgments

We acknowledge the support of the National Science Council in Taiwan through Grant No. NSC 94-2112-M-007-018. We thank Dr. K. Shiokawa for his critical reading of the manuscript.

-
- [1] L. Viola and S. Lloyd, Phys. Rev. A **58**, 2733 (1998).
 - [2] P. Zanardi, Phys. Lett. A **258**, 77 (1999).
 - [3] L. Viola, S. Lloyd, and E. Knill, Phys. Rev. Lett. **83**, 4888 (1999).
 - [4] L. Viola, E. Knill, and S. Lloyd, Phys. Rev. Lett. **82**, 2417 (1999).
 - [5] L. Viola and E. Knill, Phys. Rev. Lett. **90**, 037901(2003).
 - [6] P. Chen, Phys. Rev. A **73**, 022343 (2006).
 - [7] M. S. Byrd and D. A. Lidar, Quantum Inf. Process. **1**, 19 (2002).
 - [8] L. Viola and E. Knill, Phys. Rev. Lett. **94**, 060502 (2005).
 - [9] P. Sengupta and L. P. Pryadko, Physical Review Letters **95**, 037202(2005).
 - [10] K. Khodjasteh and D. A. Lidar, Phys Rev Lett **95**, 180501 (2005).
 - [11] P. Facchi, D. A. Lidar, and S. Pascazio, Phys. Rev. A **69**, 032314(2004).
 - [12] K. Shiokawa and D. A. Lidar, Phys. Rev. A **69**, 030302 (2004).
 - [13] L. Faoro and L. Viola, Phys. Rev. Lett. **92**, 117905 (2004).
 - [14] K. Shiokawa and B. L. Hu, e-print quant-ph/0507177 (2005).
 - [15] A. O. Caldeira and A. J. Leggett, Physica A **121**, 581 (1983).
 - [16] T. Yu, L. Diosi, N. Gisin, and W. T. Strunz, Phys. Rev. A **60**, 91 (1999).
 - [17] I. de Vega, D. Alonso, and P. Gaspard, Phys. Rev. A **71**, 023812 (2005).
 - [18] L. Diosi, N. Gisin, and W. T. Strunz, Phys. Rev. A **58**, 1699 (1998).
 - [19] T. Yu and J. H. Eberly, Phys. Rev. B **66**, 193306 (2002).
 - [20] T. Yu and J. H. Eberly, Phys. Rev. B **68**, 165322 (2003).
 - [21] W. Magnus, Commun. Pure Appl. Math. **7**, 649 (1954).
 - [22] C. Piermarocchi, P. Chen, Y. S. Dale, and L. J. Sham, Phys. Rev. B **65**, 075307 (2002).
 - [23] K. Khodjasteh and D. A. Lidar, e-print quant-ph/0607086 (2006).